Basic properties of anisotropic stellar wind expansion in the fluid approach

D. Hubert, François Leblanc

Basic properties of anisotropic stellar wind expansion in the fluid approach

D. Hubert[1]
Observatoire de Paris, Laboratoire d'Etudes Spatiale et d'Instrumentation en Astrophysique, Meudon, France

F. Leblanc
Service d'Aéronomie du CNRS/IPSL, Verrières le Buisson, France

Received 14 April 2005; revised 22 September 2005; accepted 28 September 2005; published 15 December 2005.

[1] Whereas in an isotropic temperature atmosphere both the hydrostatic equation and the momentum equation give the same conditions for hydrostatic equilibrium, in the anisotropic case the situation is ambiguous. It is found that for an anisotropic temperature the hydrostatic equilibrium conditions have to be deduced from the momentum equation. The condition for hydrostatic equilibrium is that both the parallel and the perpendicular temperatures, to the radial direction, decrease more rapidly than 1/r in the general case and that the perpendicular temperature decreases more rapidly than 1/r when the parallel temperature is constant. The momentum equation displays a transonic solution when at least one of the temperatures, parallel or perpendicular to the radial direction, decreases less rapidly than 1/r in the general case and when the perpendicular temperature decreases less rapidly than 1/r when the parallel temperature is constant. In an anisotropic atmosphere the parallel thermal velocity is the critical velocity. The properties of the transonic expansion in an isothermal and anisotropic atmosphere are studied. The initial velocity, the critical distance position, the terminal velocity, and the density profile are significantly different from the isotropic case. These properties are opposite with respect to the value of the anisotropy $T_\perp/T_\parallel > 1.0$ and $T_\perp/T_\parallel < 1.0$. In particular, for a perpendicular temperature larger than the parallel temperature the acceleration starts really at a significant distance from the base of the atmosphere, whereas the critical point is closer to the base of the atmosphere compared to the isotropic case. For an opposite anisotropy the transonic point moves far away from the base of the atmosphere, and the terminal velocity is significantly decreased for small temperature anisotropy. The mass loss rate is drastically affected for an anisotropy $T_\perp/T_\parallel > 2.0$. The extension of this study to multimoment anisotropic models can be useful for the interpretation of particle simulation of rarefied stellar atmosphere expansion.

Citation: Hubert, D., and F. Leblanc (2005), Basic properties of anisotropic stellar wind expansion in the fluid approach, *J. Geophys. Res.*, *110*, A12104, doi:10.1029/2005JA011190.

1. Introduction

[2] One of the salient features of the macroscopic state of the solar wind plasma is the temperature anisotropy of the particle populations. Recent observations on SOHO spacecraft indicate that in coronal holes the proton and the O^{5+} ion velocity distributions are anisotropic. Indeed it is deduced from self-consistent model that the temperature perpendicular to the interplanetary/solar magnetic field (IMF), $T_\perp$, is larger than the temperature parallel to that field, $T_\parallel$ [*Cranmer*, 1998; *Kohl et al.*, 1998; *Li et al.*, 1998]. In situ observations in the solar wind have shown that from 0.3 to 1 AU the proton temperature parallel and perpendicular to the IMF evolve as power laws [*Schwenn and Marsch*, 1990]. In the fast solar wind, the proton temperature anisotropy, $T_\perp/T_\parallel$, evolves from about 2.0 at 0.3 AU to about 0.8 at 1 AU (astronomical unit) in the ecliptic plane [*Schwenn and Marsch*, 1990]. A proton temperature anisotropy lower than 1.0 is also observed on Ulysses at high latitude and distances larger than 1 AU during solar minimum activity [*Feldman*, 1996]. In the slow solar wind, during minimum solar activity, the temperature anisotropy of the protons, $T_\perp/T_\parallel$, is lower than 1.0 between Mercury's orbit and the Earth's orbit as measured by Helios spacecraft [*Schwenn and Marsch*, 1990]. The electron temperature of the solar wind displays also power law evolution with the radial distance [*Pilipp et al.*, 1990]. The electron distribution functions are anisotropic at 1 AU, with the temperature perpendicular to the IMF lower than the parallel temperature [*Pilipp et al.*, 1990; *Salem et al.*, 2003].

[1] Also at Department of Chemistry, University of British Columbia, Vancouver, British Columbia, Canada.

0148-0227/05/2005JA011190

[3] The observations of proton temperature anisotropy in the lower corona and in interplanetary space with $T_\perp/T_\parallel$ larger than 1.0, as well as the observation of O^{5+} temperature anisotropy in coronal holes, provide evidence that wave-particle interactions control the distribution functions of these particles in the expansion process. If Coulomb collisions dominated, the temperature should be isotropic or such that $T_\perp < T_\parallel$ in the corona. However, the anisotropic structure of the core of the proton distribution functions observed in situ in the fast wind is a signature of perpendicular heating [*Schwenn and Marsch*, 1990], regulated by wave [*Marsch et al.*, 2004]. In the slow solar wind, observations indicate a regulation of the proton temperature anisotropy $T_\parallel > T_\perp$ through the fire hose instability [*Kasper et al.*, 2002]. The electron distribution functions observed from Helios [*Pilipp et al.*, 1987] and from WIND (C. Salem, private communication, 2003) display a typical structure with three components: the core, the halo and the strahl. The halo population is isotropic with respect to the solar wind velocity and has about 5 to 7 times the energy of the core distribution. The origin of this suprathermal halo distribution is not yet known, but is likely the result of wave-electron interaction [*Vocks et al.*, 2005]. As the halo is isotropic with respect to the solar wind velocity, the electron temperature would be more anisotropic without the halo.

[4] Without any wave-particle interaction, the temperature anisotropy of stellar atmospheres is controlled by heat conductivity and Coulomb collisions. The parallel heat conductivity, which is more important than the perpendicular heat conductivity, prevents the parallel temperature from decreasing more rapidly than the perpendicular temperature with respect to the heliocentric distance. This result has been shown for the protons for the first time by *Leer and Axford* [1972]. Recent particle simulations have shown the variation of the radial electron temperature anisotropy, $T_\perp/T_\parallel < 1.0$, with the plasma density at the base of the atmosphere in supersonic and subsonic regimes [*Landi and Pantellini*, 2003]. Coulomb collisions isotropize the particle distributions efficiently when the relaxation frequency of the anisotropy in energy ν^i is greater than the expansion rate ν_x [*Demars and Schunk*, 1979]. For a plasma composed of electrons and protons, the relaxation frequency of the energy anisotropy of the electrons is about 2.66 ν_{ee} with ν_{ee} the electron-electron collision frequency [*Demars and Schunk*, 1979]. The expansion rate of electrons is $\nu_{ex} = -(v_e/n_e)(dn_e/dr)$ in which v_e is the mean velocity of the electron population and n_e the electron density at a radial distance r. It is clear that when the density decreases the electron-electron collision frequency also decreases whereas the expansion rate increases. In such a situation Coulomb collisions become less and less efficient to maintain isotropic the electron population. For example in coronal hole at 5 R_s (solar radius), with typical electron density as well as electron temperature [*Habbal et al.*, 1995] and a velocity of 400 km s^{-1}, the anisotropic relaxation frequency is about 6.10^{-3} s^{-1} while the expansion rate is about 2.10^{-4} s^{-1}. However, with similar temperature and dynamical property in the lower corona, the anisotropic relaxation rate could be lower than the expansion rate with lower density. Regarding the protons, the relaxation frequency of the anisotropy energy is of the order $(m_e/m_p)^{1/2}$ times the relaxation frequency for the electrons, with m_e and m_p being respectively the electron and the proton mass. Therefore Coulomb collisions are less efficient to induce protons isotropy than electrons isotropy.

[5] The purpose of this paper is to study the basic properties of stellar wind atmospheres in the presence of temperature/pressure anisotropy. It is generally believed that thermal anisotropy has little effect on the dynamical properties of the solar wind but does represent an important constraint on the wave-particle interaction process [*Hu et al.*, 1997]. Nevertheless, knowledge of the processes which characterize the physical parameters of the coronal source region is important for the study of coronal heating and stellar wind formation [*Withbroe*, 1988; *Kohl et al.*, 1998; *Cranmer et al.*, 1999]. In this paper we address an anisotropic atmosphere and the conditions that are required for hydrostatic equilibrium. Then we study the nature and properties of the critical expansion solution, the profile of the expansion velocity and the mass loss rate in an anisotropic isothermal atmosphere compared to an isotropic isothermal atmosphere. We consider two kinds of anisotropy, namely $T_\perp/T_\parallel > 1.0$ typical of an atmosphere controlled by wave-particle interactions and $T_\perp/T_\parallel < 1.0$ typical of a stellar atmosphere free of wave-particle interactions and in which the Coulomb collisions do not maintain the populations in an isotropic state. In order to study the basic properties of an anisotropic expansion, we consider a one fluid approach. For the model we assume a completely ionized atmosphere composed of electrons and protons of local equal density. We consider the averaged parallel temperature to the radial direction of electrons and protons as well as the averaged perpendicular temperature. In section 2 the conditions for hydrostatic equilibrium of an anisotropic atmosphere are investigated. Section 3 addresses the expansion properties of an anisotropic isothermal atmosphere. In section 4 the results are discussed and an extension to a multimoment approach is considered. The conclusion is presented in section 5.

2. Anisotropic Stellar Atmosphere and Hydrostatic Equilibrium

[6] For the model we assume a completely ionized atmosphere with m denoting the mass of the hydrogen atom, n(r) the atomic density with respect to the radial distance r, $T_\perp(r)$ and $T_\parallel(r)$ respectively the temperatures perpendicular and parallel to the radial interplanetary magnetic field, G the gravitational constant, M_s the stellar mass and $S = r^\alpha$ the cross section of the expansion tube with $\alpha > 0$. The stellar atmosphere is governed by two basic equations: the mass conservation equation [*Parker*, 1963]:

$$\frac{d}{dr}nv + \frac{nv}{S}\frac{dS}{dr} = 0 \tag{1}$$

where v is the fluid velocity, and the momentum equation for an anisotropic pressure fluid [*Blelly and Schunk*, 1993]:

$$v\frac{d}{dr}v + \frac{2}{mn}\frac{d}{dr}\left(nkT_\parallel\right) + \frac{2k}{m}\left(T_\parallel - T_\perp\right)\frac{1}{S}\frac{d}{dr}S + \frac{GM_s}{r^2} = 0 \tag{2}$$

Comparing with the momentum equation of an isotropic fluid, we note that in the second term of equation (2) the

parallel pressure $nkT_{\parallel}$ has been substituted for the total pressure nkT, and that the third term in equation (2) contains the direct contribution of the pressure anisotropy. This contribution is proportional to the difference of the temperatures, $T_{\parallel} - T_{\perp}$, and to the index α of the cross section of the expansion tube. The larger $T_{\parallel} - T_{\perp}$ and α are, the stronger the anisotropy pressure effect is on the expansion process. We also note that for $T_{\parallel} > T_{\perp}$, the anisotropy pressure effect is usually opposite to the gradient force of the parallel pressure $d(nkT_{\parallel})/dr$, while for $T_{\perp} > T_{\parallel}$ both contributions add together to expel the plasma from the stellar gravitational attraction.

[7] Hydrostatic equilibrium requires that [*Parker*, 1963]:

$$\frac{d}{dr}\left(nkT_{\parallel}\right) + \frac{\alpha kn}{r}\left(T_{\parallel} - T_{\perp}\right) + \frac{GM_s mn}{2r^2} = 0 \tag{3}$$

If, at the base of the atmosphere, r_o, the density and the parallel temperature are n_o and $T_{\parallel o}$ respectively, the integration of equation (3) from r_o to r with $A = GM_s m/2k$ yields:

$$n(r)kT_{\parallel}(r) = n_o kT_{\parallel o} \exp\left(-\alpha \int \frac{1}{r}\left(1 - \frac{T_{\perp}}{T_{\parallel}}\right)dr - A\int \frac{dr}{T_{\parallel} r^2}\right) \tag{4}$$

[8] With an evolution law of the temperatures such that $T_{\parallel} = T_{\parallel o}(r/r_o)^{-\beta\parallel}$ and $T_{\perp} = T_{\perp o}(r/r_o)^{-\beta\perp}$ the integrals in the exponential of equation (4) are solved. Different cases are generated by the set of constant parameters $\beta_{\parallel}$ and $\beta_{\perp}$ and of the anisotropy at the base r_o of the atmosphere. Indeed:

[9] 1. If $\beta_{\parallel} \neq \beta_{\perp}$ with $\beta_{\parallel} \neq 1$

$$n(r)kT_{\parallel}(r) = n_0 kT_{\parallel 0}\left(\frac{r}{r_0}\right)^{-\alpha} \exp\left\{\frac{\alpha T_{\perp 0}}{\left(\beta_{\parallel} - \beta_{\perp}\right)T_{\parallel 0}}\left[\left(\frac{r}{r_0}\right)^{\beta_{\parallel}-\beta_{\perp}} - 1\right] - \frac{A}{r_0\left(\beta_{\parallel} - 1\right)T_{\parallel 0}}\left[\left(\frac{r}{r_0}^{\beta_{\parallel}-1} - 1\right)\right]\right\} \tag{5}$$

[10] 2. If $\beta_{\parallel} \neq \beta_{\perp}$ with $\beta_{\parallel} = 1$

$$n(r)kT_{\parallel}(r) = n_0 kT_{\parallel 0}\left(\frac{r}{r_0}\right)^{-\left(\alpha + \frac{A}{r_0 T_{\parallel 0}}\right)} \cdot \exp\left\{\frac{\alpha T_{\perp 0}}{(1-\beta_{\perp})T_{\parallel 0}}\left[\left(\frac{r}{r_0}\right)^{1-\beta_{\perp}} - 1\right]\right\} \tag{6}$$

[11] 3. If $\beta_{\parallel} = \beta_{\perp}$ with $\beta_{\parallel} \neq 1$

$$n(r)kT_{\parallel}(r) = n_0 kT_{\parallel 0}\left(\frac{r}{r_0}\right)^{-\alpha\left(1 - \frac{T_{\perp 0}}{T_{\parallel 0}}\right)} \cdot \exp\left\{-\frac{A}{r_0\left(\beta_{\parallel} - 1\right)T_{\parallel 0}}\left[\left(\frac{r}{r_0}\right)^{\beta_{\parallel}-1} - 1\right]\right\} \tag{7}$$

[12] 4. If $\beta_{\parallel} = \beta_{\perp}$ with $\beta_{\parallel} = 1$

$$n(r)kT_{\parallel}(r) = n_0 kT_{\parallel 0}\left(\frac{r}{r_0}\right)^{-\alpha\left(1 - \frac{T_{\perp 0}}{T_{\parallel 0}}\right) - \frac{A}{r_0 T_{\parallel 0}}} \tag{8}$$

[13] The total pressure n(r)kT(r) is obtained from the parallel pressure $n(r)kT_{\parallel}(r)$ by using the relation for the average temperature T(r) in terms of the parallel and the perpendicular temperatures that is $T(r) = (T_{\parallel}(r) + 2T_{\perp}(r))/3$. It is easy to check that as r increases to infinity the total pressure decreases to zero or remains finite, similarly to the parallel pressure for the above 4 cases. The pressure decreases to zero as r increases to infinity for various values of the parameters $\beta_{\parallel}$ and $\beta_{\perp}$. Indeed this property is verified for: 1) $\beta_{\parallel} < \beta_{\perp}$, 2) $\beta_{\parallel} > \beta_{\perp}$ with $\beta_{\parallel} > 1$ and $\beta_{\perp} > 1$ or with $\beta_{\perp} = 1.0$ and $\alpha T_{\perp o} < A/r_o$, 3) $\beta_{\parallel} = \beta_{\perp}$ with $\beta_{\parallel} > 1.0$ or with $\beta_{\parallel} < 1.0$ and $T_{\perp o}/T_{\parallel o} < 1.0$ or with $\beta_{\parallel} = 1.0$ and $\alpha(T_{\perp o} - T_{\parallel o}) < A/r_o$.

[14] Let us consider the case with $\beta_{\parallel} < \beta_{\perp}$ and $\beta_{\parallel} < 1.0$ for which n(r)kT(r) goes to zero as r goes to infinity, as obtained from equation (5). Using the mass conservation equation (1), the momentum equation (2) becomes:

$$\frac{1}{v}\frac{d}{dr}v = \left(\alpha\frac{a_{\perp}^2}{r} + \beta_{\parallel}\frac{a_{\parallel}^2}{r} - \frac{GM_s}{r^2}\right)\Big/\left(v^2 - a_{\parallel}^2\right) \tag{9}$$

where $a_{\perp}^2 = 2kT_{\perp}/m$, $a_{\parallel}^2 = 2kT_{\parallel}/m$. As $T_{\parallel}$ (r) decreases less rapidly than 1/r and as long as at the base of the atmosphere $\alpha a_{\perp}^2 + \beta_{\parallel} a_{\parallel}^2 < GM_s/r_o$, a critical point $r_c > r_o$ exists with $r_c = GM_s/(\alpha a_{\perp c}^2 + \beta_{\parallel} a_{\parallel c}^2)$ where $a_{\perp c}^2 = a_{\perp}^2(r_c)$ and $a_{\parallel c}^2 = a_{\parallel}^2(r_c)$. A transcritical solution exists with $v(r_c) = a_{\parallel}(r_c)$ if at r_o the velocity is $v(r_o) \ll a_{o\parallel}(r_o)$ and at large distance $r \gg r_c$, $v(r) \gg a_{\parallel}(r_c)$, and if the slope of the velocity in r_c is positive. The slope of the velocity at the critical point r_c is:

$$\left(\frac{dv}{dr}\right)_{r_c} = \frac{1}{2}\left(-\frac{\beta_{\parallel} a_{\parallel c}}{2r_c} \pm \left[\left(\frac{\beta_{\parallel} a_{\parallel c}}{2r_c}\right)^2 + 2\alpha(1-\beta_{\perp})\frac{a_{\perp c}^2}{r_c^2} + 2\beta_{\parallel}\left(1 - \beta_{\parallel}\right)\frac{a_{\parallel c}^2}{r_c^2}\right]^{1/2}\right) \tag{10}$$

From the derivatives of the curves GM_s/r and $\alpha a_{\perp}^2 + \beta_{\parallel} a_{\parallel}^2$ at the intersection point r_c one obtains:

$$\frac{d}{dr}\left(\frac{GM_s}{r}\right)_{r_c} < \frac{d}{dr}\left(\alpha a_{\perp}^2 + \beta_{\parallel} a_{\parallel}^2\right)_{r_c} \tag{11}$$

and then $\alpha(1 - \beta_{\perp})a_{\perp c}^2 + \beta_{\parallel}(1 - \beta_{\parallel})a_{\parallel c}^2 > 0$. With this relation included in equation (10), it is shown that $(dv/dr)_{rc}$ has a positive and a negative value. Therefore the analysis based on the momentum equation predicts a transcritical solution, while the analysis of the hydrostatic equation for the same temperature law predicts the decreasing of the pressure to zero at large distance.

[15] Another case is considered with $\beta_{\parallel} = \beta_{\perp}$ and $\beta_{\parallel} < 1.0$ with a constant temperature anisotropy determined at the base of the atmosphere by $T_{\perp o}/T_{\parallel o}$. From equation (7) it is clear that for $T_{\perp o}/T_{\parallel o} \geq 1.0$ the parallel pressure and therefore the total pressure is finite or increases to infinity as $r \rightarrow \infty$. However, for $T_{\perp o}/T_{\parallel o} < 1.0$ the pressure decreases to zero for $r \rightarrow \infty$ as already indicated. We note that the momentum equation (9) does not contain any condition on the temperature anisotropy $T_{\perp o}/T_{\parallel o}$. As long as at the base of the atmosphere the relation $\alpha a_{\perp}^2 + \beta_{\parallel} a^2{}_{\parallel} < GM_s/r_o$ is verified, a critical point is determined because $\alpha a_{\perp}^2 + \beta_{\parallel} a_{\parallel}^2$

decreases less rapidly than 1/r. From equation (10), with $\beta_{\|} = \beta_{\perp} < 1.0$, it is directly obtained that the slope of the velocity at the critical point has a positive and a negative value. Therefore all the conditions are verified for the existence of a transcritical solution with $v(r_c) = a_{\|}(r_c)$. The isothermal case with $\beta_{\|} = \beta_{\perp} = 0$ and $T_{\perp o}/T_{//o} < 1.0$ is a particular case which will be extensively discussed in section 3.

[16] We conclude that when the parallel temperature decreases smoothly with $\beta_{\perp} \geq \beta_{\|}$ and $\beta_{\|} < 1.0$ or with $0 < \beta_{\|} = \beta_{\perp} < 1.0$ and $T_{\perp o}/T_{\|o} < 1.0$, the atmosphere cannot be longer bounded by the gravitational field. This result is coherent with the substitution of the gradient of the parallel pressure to the gradient of the total pressure in the momentum equation (2). The gradient of the parallel pressure appears to be the leading force, while the gradient of the perpendicular pressure is a complementary force. The anisotropic isothermal case, with $\beta_{\|} = \beta_{\perp} = 0.0$ and $T_{\perp o}/T_{\|o} < 1.0$, corresponds to an atmosphere heated on a large extend whatever the anisotropy. In this situation, the atmosphere is no more bounded by the gravitational field. We note that for the above values of the parameters $\beta_{\|}$ and $\beta_{\perp}$, the pressure decreases as a power law rather than as an exponential law, implying a very low-pressure decay at large distances.

[17] From these case studies we conclude that the conditions for a static atmosphere derived from the hydrostatic equilibrium requirement is not valid for anisotropic atmospheres. The momentum equation (9) sheds some new aspects on the transonic solution. In the general case of an anisotropic atmosphere the condition for a static atmosphere is that the quantity $\alpha T_{\perp}$ (r) + $\beta_{\|} T_{\|}$ (r) decreases more rapidly than 1/r. This condition implies that both $T_{\perp}$(r) and $T_{\|}$ (r) have to decrease more rapidly than 1/r, except in the particular case of a constant parallel temperature, where $T_{\perp}$(r) has to decrease more rapidly than 1/r for a static atmosphere. The conditions for a transonic expansion are directly obtained in the general case, when $T_{\perp}$(r) or $T_{\|}$(r) decreases less rapidly than 1/r and in the particular case of a constant parallel temperature when the perpendicular temperature decreases less rapidly than 1/r. In the transonic solution we note that the critical velocity is the parallel thermal velocity, $v_c = a_{\|}$, while the critical point, $r_c = GM_s/(\alpha a_{\perp}^2 + \beta_{\|} a_{\|}^2)$, is determined from contributions of the parallel and the perpendicular thermal velocities in the general case. In the particular case of a constant parallel temperature, the critical point is determined from the perpendicular thermal velocity only, that is, $r_c = GM_s/\alpha a_{\perp}^2$. These conditions generalize the condition derived for an isotropic atmosphere expansion [*Parker*, 1963].

3. Expansion of an Anisotropic Isothermal Atmosphere

[18] In this section we study the expansion of an isothermal atmosphere with a constant temperature anisotropy that is with $\beta_{\|} = \beta_{\perp} = 0$. The momentum equation (9) is therefore:

$$\frac{1}{v}\frac{d}{dr}v = \left(\frac{\alpha a_{\perp}^2}{r} - \frac{GM_s}{r^2}\right) \Big/ \left(v^2 - a_{\|}^2\right) \tag{12}$$

We have already considered the conditions at the base, r_o, and at large radial distance for the transcritical solution. The critical point and the critical velocity which are respectively $r_c = GM_s/\alpha a_{\perp}^2$ and $v_c = a_{\|}$ are dependent on the anisotropic temperature. From the relations between the parallel temperature, the perpendicular temperature and the average temperature of the atmosphere, $T = (T_{\|} + 2T_{\perp})/3$, we deduce new expression of the critical distance:

$$r_c = \frac{r_{ci}}{3}\left(2 + \frac{T_{\|}}{T_{\perp}}\right) \tag{13}$$

and of the critical velocity:

$$v_c = 3^{1/2} a_i \left(1 + 2T_{\perp}/T_{\|}\right)^{-1/2} \tag{14}$$

in which r_{ci} and a_i are respectively the critical distance and the critical velocity of an isotropic and isothermal wind at the average temperature T. At the critical point, the slope of the velocity is:

$$\left(\frac{dv}{dr}\right)_{r_c} = \frac{\alpha^{3/2}}{2^{1/2}} \frac{a_{\perp}^3}{GM_s} \tag{15}$$

or

$$\left(\frac{dv}{dr}\right)_{r_c} = 3^{3/2}\left(2 + \frac{T_{\|}}{T_{\perp}}\right)^{-\frac{3}{2}} \left(\frac{dv}{dr}\right)_{r_{ci}} \tag{16}$$

where the velocity slope is expressed in terms of the temperature anisotropy and the slope of the velocity at the critical point $(dv/dr)r_{ci}$ of an equivalent isotropic atmosphere at temperature T.

[19] For an anisotropy such that $T_{\perp} > T_{\|}$, the above expressions show that the critical distance and the critical velocity are smaller than in the equivalent isotropic atmosphere at average temperature T, while the slope of the velocity at the critical point is larger than in the equivalent isotropic atmosphere. In the limit of very high temperature anisotropy, $T_{\perp} \gg T_{\|}$, the critical distance reaches the limit $r_c = 2r_{ci}/3$, while the critical velocity decreases to zero. In the same limit of large temperature anisotropy, the slope of the velocity at the critical point also reaches a limit which is $(3/2)^{3/2}$ larger than the velocity slope at the critical point of an equivalent isotropic atmosphere at temperature T.

[20] For the opposite temperature anisotropy, $T_{\perp} < T_{\|}$, the critical point is at a larger distance and the critical velocity is larger than in the isotropic case as deduced respectively from equation (13) and equation (14). From equation (16), we note that the slope of the velocity at the critical point decreases with respect to the isotropic case. In the limit of $T_{\perp} \ll T_{\|}$, the critical point is rejected to infinity, while the critical velocity reaches the value $v_c = 3^{1/2} a_i$. In the same limit, as $T_{\perp} \to 0$, then $T_{\|} \approx 3T$, and from equation (16) one derives that the slope of the velocity at the critical point tends to zero.

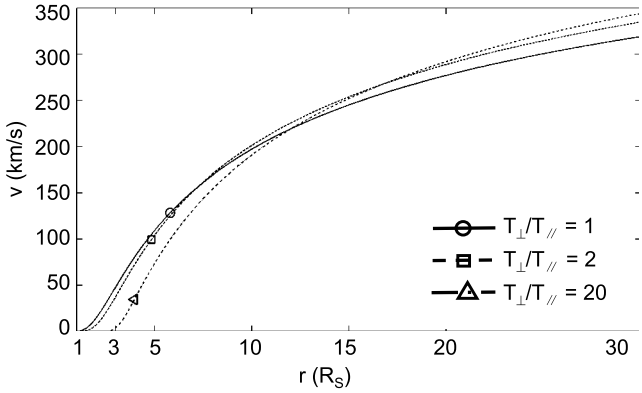

Figure 1. Velocity profiles in the range of 1 to 30 R_s for 3 temperature anisotropies $T_\perp/T_\parallel > 1.0$. The circle, the square, and the triangle indicate the position and the velocity of the critical point for temperature anisotropy equal to 1.0, 2.0, and 20.0, respectively.

3.1. Velocity Profiles of the Critical Solution

[21] The analytical expression for the velocity is obtained from equation (12) with use of the condition $v_c = a_\parallel$ at the critical point r_c. The solution is:

$$v \exp\left(-\frac{v^2}{2a_\parallel^2}\right) = a_\parallel \left(\frac{r_c}{r}\right)^{\alpha\frac{T_\perp}{T_\parallel}} \exp\left[\alpha\frac{T_\perp}{T_\parallel}\left(1-\frac{r_c}{r}\right)-\frac{1}{2}\right] \qquad (17)$$

The initial velocity at the base of the atmosphere is obtained by applying equation (17) at r_o. With $v_o \ll a_\parallel$ one obtains:

$$v_0 \approx a_\parallel \left(\frac{r_c}{r_0}\right)^{\alpha\frac{T_\perp}{T_\parallel}} \exp\left[\alpha\frac{T_\perp}{T_\parallel}\left(1-\frac{r_c}{r_0}\right)-\frac{1}{2}\right] \qquad (18)$$

[22] Equation (17) is solved numerically. In Figures 1 and 2 velocity profiles are presented for a spherical expansion of an atmosphere with anisotropies $T_\perp/T_\parallel \geq 1$. Typically, we consider a stellar mass and a stellar radius equal respectively to the mass and to the radius of the Sun. These profiles have been obtained from equation (17) with an isothermal temperature of 10^6 K, and 3 values of the temperature anisotropy $T_\perp/T_\parallel$, equal to 1.0, 2.0 and 20. Figure 1 displays the velocity profiles from the base of the atmosphere at $r_o = 1.0$ R_s to 30 R_s in which R_s is the Sun radius. In this figure we note that as the temperature anisotropy increases, the velocity v_o at the base r_o of the atmosphere decreases toward zero. It is also observed that for large temperature anisotropy the expansion velocity has very small values between r_o and the critical point r_c. The critical velocity and the critical distance both decrease with respect to the values of the isotropic case which are respectively 128 km/s and 6.9 R_s. For $T_\perp/T_\parallel = 2.0$ the critical velocity is 100 km/s and the critical point is at about 5 R_s while for $T_\perp/T_\parallel = 20$, the critical velocity is some 30 km/s and the critical point is less than 4 R_s. In the lower corona for distances lower than some 9 R_s, the expansion velocity is lower than the velocity in the isotropic case but for distances larger than some 10 R_s the expansion velocity increases with increasing anisotropy.

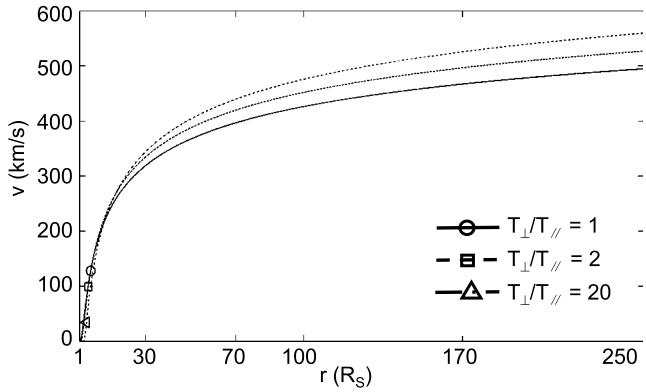

Figure 2. Velocity profiles at large distances in the range of 1 to 250 R_s for three temperature anisotropies $T_\perp/T_\parallel$ equal to 1.0, 2.0, and 20.0.

[23] Figure 2 displays the velocity profiles at large distances from the base of the atmosphere. It is noted that at a given distance from the base of the atmosphere, the effect of the anisotropy on the expansion velocity is not very important and saturates rapidly when the anisotropy increases to large values. For example, for a very high anisotropy $T_\perp/T_\parallel = 20$, the expansion velocity at 1 AU is only 60 km/s larger than in the isotropic case. As the distance from the base of the atmosphere increases, the expansion velocity increases to infinity, as shown from the formula:

$$v(r \to \infty) \cong a_\parallel \left(2\alpha\frac{T_\perp}{T_\parallel}\log\frac{r}{r_c}\right)^{1/2} \qquad (19)$$

This is derived from the velocity formula equation (17) in the limit of large distance from the base r_o.

[24] Let us consider now the case of a small temperature anisotropy, $T_\perp/T_\parallel < 1.0$. In Figure 3 and 4 the velocity profiles have been calculated for an isothermal temperature of 10^6 K, and 3 values of the temperature anisotropy $T_\perp/T_\parallel$ equal to 1.0, 0.5, and 0.05. In this case of anisotropy with

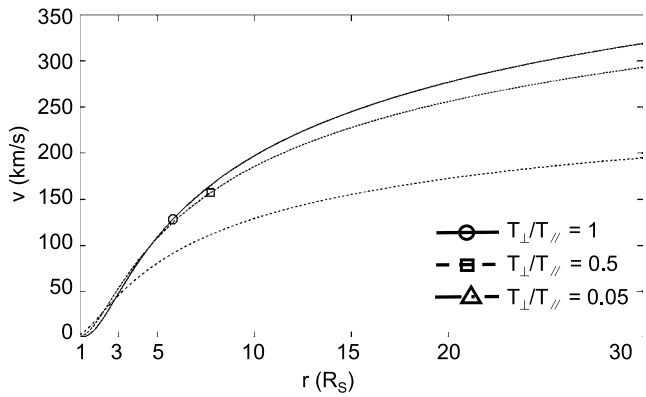

Figure 3. Velocity profiles in the range of 1 to 30 R_s for three temperature anisotropies $T_\perp/T_\parallel < 1.0$. The circle and the square indicate the position and the velocity of the critical point for temperature anisotropy equal to 1.0 and 0.5, respectively. For a temperature anisotropy equal to 0.05 the critical point is father than 30 R_s from the base of the atmosphere.

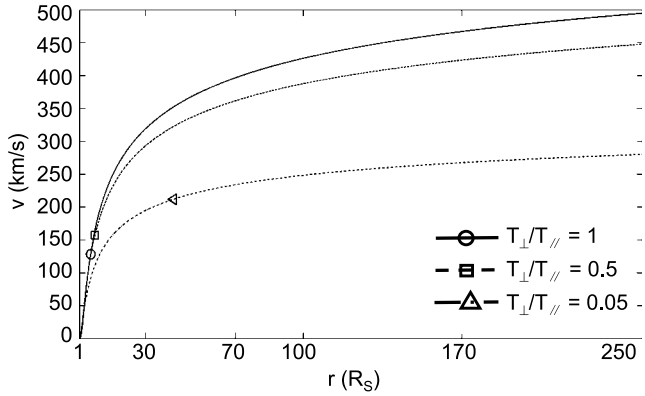

Figure 4. Velocity profiles at large distances in the range of 1 to 250 R_s for three temperature anisotropies $T_\perp/T_\parallel$ equal to 1.0, 0.5, and 0.05. The critical point for the anisotropy equal to 0.05 is at 50 R_s.

$T_\perp/T_\parallel < 1.0$ the expansion process shows characteristics that are different than in the case of anisotropy with $T_\perp/T_\parallel > 1.0$. Indeed, in the case of small anisotropy it is observed in Figure 3, that the velocity at the base r_o, the critical velocity and the critical distance are larger than the respective values in the case of high anisotropy. For a very low anisotropy equal to 0.05 the critical point is at some 50 R_s and the critical velocity is 215 km/s as seen in Figure 4. In the limit of $T_\perp/T_\parallel \rightarrow 0$ the initial velocity v_o tends to $3^{1/2}a_i \exp(-\alpha r_{ci}/3r_o - 1/2)$.

[25] At large distances it is shown that the expansion velocity is very sensitive to the anisotropy $T_\perp/T_\parallel \leq 1.0$. For example, at 1 AU for an anisotropy of 0.05 the velocity is about half of the value obtained in the isotropic case at the same average temperature. The numerical results illustrated in Figure 4 are consistent with the theoretical results derived from the formulas which show that the critical point is displaced to infinity, the slope of the velocity at the critical point tends to zero while the critical velocity approaches $v_c = 3^{1/2}a_i$ for a temperature anisotropy decreasing to zero. In the same limit of decreasing temperature anisotropy, one derives from equation (17), that at large distance $r \geq r_c$ the terminal velocity $v(r \rightarrow \infty)$ approaches the critical velocity $3^{1/2}\ a_i$.

3.2. Density Profile and the Mass Loss Rate

[26] The density profile is obtained from the mass conservation equation (1) which after direct calculations yields

$$n(r) = n_0 \left(\frac{r}{r_0}\right)^{\alpha\left(\frac{T_\perp}{T_\parallel}-1\right)} \exp\left[-\frac{v^2}{2a_\parallel^2}\right] \exp\left[-\frac{GM_s}{a_\parallel^2}\left(\frac{1}{r_0}-\frac{1}{r}\right)\right] \tag{20}$$

In a static isothermal atmosphere with constant temperature anisotropy, the density derived from the hydrostatic equation (3) is

$$n(r) = n_0 \left(\frac{r}{r_0}\right)^{\alpha\left(\frac{T_\perp}{T_\parallel}-1\right)} \exp\left[-\frac{GM_s}{a_\parallel^2}\left(\frac{1}{r_0}-\frac{1}{r}\right)\right] \tag{21}$$

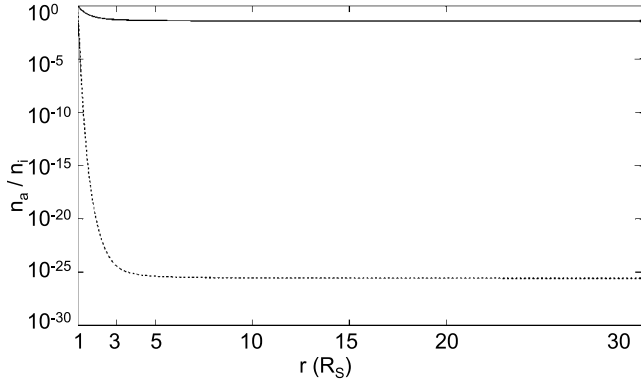

Figure 5. Density profiles for temperature anisotropy equal to 2.0 (solid line) and 20.0 (dashed line) compared to the density profile for the isotropic case.

We note that the two profiles of the density equations (20) and (21) are similar. They are very close at the bottom of the atmosphere for distances lower than the critical distance r_c.

[27] The ratio of the density in an anisotropic isothermal stellar wind, n_a, to the density in an isotropic isothermal wind, n_i, is given by

$$\frac{n_a}{n_i} = \left(\frac{r}{r_0}\right)^{\alpha\left(\frac{T_\perp}{T_\parallel}-1\right)} \exp\left(\frac{v_i^2}{2a_i^2} - \frac{v_a^2}{2a_\parallel^2}\right) \cdot \exp\left[-GM_s\left(\frac{1}{a_\parallel^2}-\frac{1}{a_i^2}\right)\left(\frac{1}{r_o}-\frac{1}{r}\right)\right] \tag{22}$$

Figures 5 and 6 show the evolution of the density ratios n_a/n_i of a spherical expansion from the base of the atmosphere to 30 R_s for different values of the temperature anisotropy and an average temperature of 10^6 K. For temperature anisotropy $T_\perp/T_\parallel$ equal to 2.0 and 20 the density ratios in Figure 5 are seen to be lower than 1.0. The larger $T_\perp/T_\parallel$ is, the lower is n_a/n_i. In particular, the ratio decreases strongly until a few stellar radii and for a large anisotropy the ratio is very small. For an opposite temperature anisotropy with $T_\perp/T_\parallel \leq 1.0$ the ratio n_a/n_i is larger than 1 as seen in Figure 6. This ratio increases smoothly until a few stellar radii.

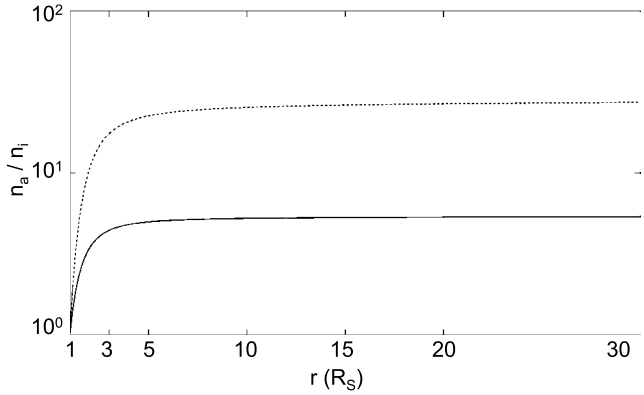

Figure 6. Density profiles for temperature anisotropy equal to 0.5 (solid line) and 0.05 (dashed line) compared to the density profile for the isotropic case.

[28] The mass loss rate can be estimated from the density and the velocity at the critical point. For a spherical expansion one gets the expression, $M_a = 4\pi n(r_c)a_{\|}$, that is more explicitly

$$M_a = 4\pi n_o a_{\|} r_c^2 \left(\frac{r_c}{r_o}\right)^{\alpha\left(\frac{T_\perp}{T_{\|}}-1\right)} \exp\left[-\frac{GM_s}{a_{\|}^2}\left(\frac{1}{r_o}-\frac{1}{r_c}\right)-\frac{1}{2}\right] \quad (23)$$

For a spherical expansion, the ratio of the mass loss rate of an anisotropic atmosphere to the mass loss rate of an isotropic atmosphere at the same temperature is:

$$\frac{M_a}{M_i} = \frac{a_{\|}}{9a_i}\left(2+\frac{T_{\|}}{T_\perp}\right)^2 \left(\frac{r_{ca}}{r_o}\right)^{2\left(\frac{T_\perp}{T_{\|}}-1\right)} \cdot \exp\left[-\frac{GM_s}{r_o}\left(\frac{1}{a_{\|}^2}-\frac{1}{a_i^2}\right)+2\left(\frac{T_\perp}{T_{\|}}-1\right)\right] \quad (24)$$

[29] Figure 7 displays the ratio of the mass loss rate of an isothermal anisotropic atmosphere in a spherical expansion to an isotropic spherical expansion at the same temperature, for anisotropies $T_\perp/T_{\|}$, equal to 0.05 to 20. For the low temperature anisotropy, the mass loss rate is about 10 times higher than in the isotropic case and not sensitive to the anisotropy. However, for anisotropy larger than 2, the mass loss rate decreases significantly and is very sensitive to the anisotropy value.

4. Discussion

[30] The study of the expansion of an anisotropic stellar atmosphere displays properties which are different from the isotropic case. We have shown that the hydrostatic equation of an anisotropic atmosphere does not provide the conditions for the atmosphere to be maintained in a static equilibrium. Indeed, we have found sets of the parallel and perpendicular temperature laws, with $\beta_\perp > \beta_{\|}$ and $\beta_{\|} < 1.0$ or $\beta_{\|} = \beta_\perp$ with $\beta_{\|} < 1.0$ and the anisotropy $T_{\perp o}/T_{\|o} < 1.0$ at the base of the atmosphere, for which the pressure decreases to zero at large radial distance, but for which a transcritical solution of the momentum equation is obtained. This result shows that the condition that the pressure decreases to zero at large distance is not a sufficient condition for an anisotropic atmosphere to be in hydrostatic equilibrium. Therefore as stressed by *Velli* [2001], the condition for a supersonic flow on the basis of pressure argument only does not appear to be as definitive. This discrepancy is related to the mirror force resulting from the anisotropic pressure and which is proportional to $T_\perp - T_{\|}$. For temperature anisotropy such that $T_\perp/T_{\|} < 1.0$ the mirror force drives the pressure to zero at large distances but is not efficient enough to prevent the atmosphere from expanding for the above specific conditions. It is interesting to note that the set of parameters, $\beta_\perp > \beta_{\|}$ with $\beta_{\|} < 1.0$, corresponds to realistic stellar atmosphere.

[31] The conditions for an anisotropic atmosphere to be in hydrostatic equilibrium are that both the parallel and the perpendicular temperature decrease more rapidly than 1/r in the general case. In the case of a constant parallel temperature the condition is that the perpendicular temperature decrease more rapidly than 1/r. The condition for a supercritical expansion is therefore that, either the parallel or the perpendicular temperature, decreases less rapidly than 1/r in the general case. In the case of a constant parallel temperature, the condition is that the perpendicular temperature decreases less rapidly than 1/r. These conditions generalize the one obtained in the case of an isotropic atmosphere [*Parker*, 1963].

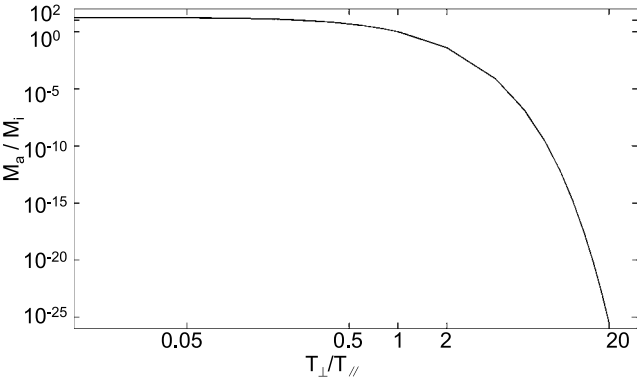

Figure 7. Mass loss rate for temperature anisotropy in the range 0.05 to 20.0 compared to the mass loss rate in the temperature isotropic case.

[32] The effects of the temperature anisotropy on the expansion properties of an isothermal atmosphere are significant. For a constant anisotropy with $T_\perp/T_{\|} > 1.0$, the distance to the critical point and the critical velocity are smaller than for an isotropic atmosphere at the same temperature, while for an anisotropy with $T_\perp/T_{\|} < 1.0$, the distance to the critical point and the critical velocity are larger than in an isotropic atmosphere. In the limit of very high and very low temperature anisotropy, asymptotic limits to the critical point position and to the critical velocity are obtained. In particular in the limit of very high anisotropy, the critical point is at 2/3 of the critical distance of the equivalent isotropic case at the same temperature, and the critical velocity decreases to zero. The velocity at the base of the atmosphere of the critical solution decreases to zero with an increasing anisotropy, and so does the velocity between the base of the atmosphere and the position of the critical point. This result shows that for an isothermal atmosphere with high temperature anisotropy, the expansion does not really start at the base of the atmosphere, but at a significant distance from the base. In this case the acceleration is violent. In the limit of the anisotropy going to zero the critical point is displaced to an infinite distance and the critical velocity approaches $(3/2)^{1/2}$ a_i with a_i being the thermal velocity at temperature T. Similar effects of the temperature anisotropy of an isothermal atmosphere on the position of the critical point can be easily extended to the case of an atmosphere with $\beta_{\|} = \beta_\perp < 1.0$. These results show that the effects of additional momentum or energy in a lower stellar corona will depend on the anisotropic state of the atmosphere through the position of the critical point [*Lamers and Cassinelli*, 1999].

[33] The numerical solution of the isothermal model with a constant anisotropy along the radial distance, shows that the velocity profiles with anisotropies larger and smaller than one are quite different. For an anisotropy $T_\perp/T_{\|} > 1.0$,

the velocity in the lower atmosphere until about 9 R_s is smaller than in the isotropic case for the same average temperature. At large distances the velocity profiles saturate rapidly with increasing anisotropy. At a given distance, the anisotropy effect on the expansion velocity is not important even for very high anisotropy as already stressed by *Hu et al.* [1997]. For anisotropy with $T_\perp/T_\parallel > 1.0$ the velocity increases infinitely with increasing radial distance. For anisotropy $T_\perp/T_\parallel < 1.0$ the profile of the velocity is very sensitive to the anisotropy. At large distance, the velocity is much smaller than in the isotropic case. For $T_\perp/T_\parallel$ decreasing to zero, the velocity at large distance approaches the critical velocity which is $(3/2)^{1/2}$ larger than the thermal velocity a_i of the atmosphere. This shows that for decreasing anisotropy to zero, the velocity does not increase infinitely at large distance.

[34] The density profile of an isothermal atmosphere is drastically affected by the anisotropy of the temperature. For $T_\perp/T_\parallel > 1.0$ the density n_a is lower than the density n_i in the isotropic case. The ratio n_a/n_i decreases drastically for increasing anisotropy in the lower atmosphere and become rather constant at distances larger than about 3 R_s. For $T_\perp/T_\parallel < 1.0$ the ratio n_a/n_i is moderately higher than in the isotropic case and is not greatly affected by the decreasing anisotropy. The mass loss rate in an isothermal atmosphere is drastically reduced with respect to the isotropic case for increasing anisotropy $T_\perp/T_\parallel$ larger than 2.0, but is a little larger for anisotropy $T_\perp/T_\parallel < 1.0$ whatever the value of the anisotropy.

[35] A two fluid theory [*Leer and Axford*, 1972] or a multimoment approach, which accounts for a non-Maxwellian state of the particles [*Blelly and Schunk*, 1993; *Leblanc et al.*, 2000; *Li*, 1999], can be used to describe a stellar atmosphere with different temperature laws for electrons and protons. In a multimoment approach, the electrostatic field that regulates the quasi-neutrality and the zero electric current, is the ambipolar electric field [*Blelly and Schunk*, 1993]. The electrostatic field is derived from the electron momentum equation for a nonequilibrium stationary state. Through the polynomial development of the distribution function, at 8 or 13 moment order for example, nonequilibrium contributions are included in the electrostatic field definition, such as the thermal diffusion effect [*St-Maurice and Schunk*, 1976]. These contributions result from the electron-proton momentum collisional transfer. The proton momentum equation is then considered within the electrostatic field. As the total momentum collisional transfer between electrons and protons is conserved, the proton momentum equation does not contain collisional contributions contrary to the relevant equations in the work of *Blelly and Schunk* [1993]. Under the assumption that the flow velocity of the protons is the flow velocity of the stellar wind, the momentum equation for the protons takes a similar form as the momentum equation in the one fluid approach, that is:

$$\frac{1}{v_p}\frac{d}{dr}v_p = \left(\frac{\alpha}{2r}\left[a_{p\perp}^2 + a_{e\perp}^2\right] + \frac{1}{2r}\left[\beta_{p\parallel}a_{p\parallel}^2 + \beta_{e\parallel}a_{e\parallel}^2\right] - \frac{GM_s}{r^2}\right) \Big/ \left(v^2 - \frac{1}{2}\left[a_{p\parallel}^2 + a_{e\parallel}^2\right]\right) \quad (25)$$

with $a_{p\perp}^2 = 2kT_{p\perp}/m_p$, $a_{e\perp}^2 = 2kT_{e\perp}/m_p$, $a_{p\parallel}^2 = 2kT_{p\parallel}/m_p$ and $a_{e\parallel}^2 = 2kT_{e\parallel}/m_p$ in which m_p is the proton mass. The necessary and sufficient condition for a transcritical solution is that at least one of the anisotropic temperatures of the protons or the electrons, decreases less rapidly than 1/r in the case where the two parallel temperatures are not constant. In the case where the two parallel temperatures are constant, one of the perpendicular temperatures has to decrease less rapidly than 1/r to obtain a transcritical solution. The critical velocity is therefore $v_c = ([a_{p\parallel}^2 + a_{e\parallel}^2]/2)^{1/2}$ and the critical point $r_c = 2GM_s/(\alpha[a_{p\perp}^2 + a_{e\perp}^2] + [\beta_{p\parallel}a_{p\parallel}^2 + \beta_{e\parallel}a_{e\parallel}^2])$.

[36] Recent particle simulations of a rarefied stellar atmosphere have shown that the proton parallel thermal velocity plays a particular role in the interpretation of the results [*Landi and Pantellini*, 2003]. It was also concluded, that with decreasing collisions, the acceleration efficiency decreases because the electron heat flux needs sufficient collisions to be converted efficiently into bulk atmospheric velocity. Unfortunately, these simulations limited to 50 R_s do not show the proton temperature evolution. Our results shed light on these simulations. They show first, that the parallel thermal velocity of the particles appears to be directly related to the critical velocity in the transcritical solution. Second, the parallel heat conductivity, which is more important than the perpendicular heat conductivity, prevents the parallel temperature from decreasing more rapidly than the perpendicular temperature with the radial distance [*Leer and Axford*, 1972]. For atmospheres, with a lower collision frequency, the heat conductivity decreases [*Bell et al.*, 1981] while the perpendicular temperature is more decoupled from the parallel temperature and decreases more rapidly with radial distance [*Phillips and Gosling*, 1990]. In such a case, the critical point moves away from the base of the atmosphere because the temperature anisotropy of the two populations of the atmosphere continuously decreases.

5. Conclusion

[37] In conclusion, this study shows that the basic properties of an anisotropic stellar atmosphere are specific. It has been shown that the decrease of the pressure toward zero at large distance does not provide the condition for an anisotropic atmosphere to be in hydrostatic equilibrium. The momentum equation has to be considered in order to define the conditions for a hydrostatic equilibrium as well as to define the conditions for a transcritical expansion.

[38] The solution of the anisotropic isothermal one fluid model displays new properties of the initial velocity, the critical velocity and the critical point as well as of the terminal velocity and the mass loss rate. The momentum equation for an atmosphere composed of electrons and protons with different temperature anisotropies is the same in the two fluid and multimoment approach. This equation plays a central role in understanding the expansion of a stellar atmosphere with different temperature components as well as in the illustration of particle simulations of rarefied stellar atmospheres.

[39] **Acknowledgments.** D. Hubert is grateful for the hospitality extended to him at the Department of Chemistry of the British Columbia

University. This author thanks warmly B. Shizgal for deep discussions on fundamental issues in kinetic theory, as well as G. Atkinson for pertinent questions.

[40] Shadia Rifai Habbal thanks Simone Landi and another referee for their assistance in evaluating this paper.

References

Bell, A. R., R. G. Evans, and D. J. Nicholas (1981), Electron energy transport in steep temperature gradient in laser-produced plasmas, *Phys. Rev. Lett.*, *46*, 243.

Blelly, P. L., and R. W. Schunk (1993), A comparative study of the time-dependent standard 8-, 13- and 16-moment transport formulations of the polar wind, *Ann. Geophys.*, *11*, 443.

Cranmer, S. R. (1998), Non-Maxwellian redistribution in solar coronal Lyα emission, *Astrophys. J.*, *508*, 925.

Cranmer, S. R., et al. (1999), An empirical model of a polar coronal hole at solar minimum, *Astrophys. J.*, *511*, 481.

Demars, H. G., and R. W. Schunk (1979), Transport equations for multi-species plasmas based on individual bi-Maxwellian distributions, *J. Phys. D Appl. Phys.*, *12*, 1051.

Feldman, W. C. (1996), Constraint on high-speed solar wind structure near its coronal base: A Ulysses perspective, *Astron. Astrophys.*, *316*, 355.

Habbal, S. R., R. Esser, M. Guhathakurta, and R. Fisher (1995), Flow properties of the solar wind derived from a two-fluid model with constraints from light and in situ interplanetary observations, *Geophys. Res. Lett.*, *22*, 1465.

Hu, Y. Q., R. Esser, and S. Habbal (1997), A fast solar wind model with anisotropic proton, *J. Geophys. Res.*, *102*, 14,661.

Kasper, J. C., A. J. Lazarus, and S. P. Gary (2002), Wind/SWE observations of firehose constraint on solar wind proton temperature anisotropy, *Geophys. Res. Lett.*, *29*(17), 1839, doi:10.1029/2002GL015128.

Kohl, J. L., et al. (1998), UVCS/SOHO empirical determinations of anisotropic velocity distributions in the solar corona, *Astrophys. J.*, *501*, L127.

Lamers, H. J. G. L., and J. P. Cassinelli (1999), *Introduction to Stellar Winds*, Cambridge Univ. Press, New York.

Landi, S., and F. Pantellini (2003), Kinetic simulations of the solar wind from the subsonic to the supersonic regime, *Astron. Astrophys.*, *400*, 769.

Leblanc, F., D. Hubert, and P. L. Blelly (2000), Comparison of generalized and bi-Maxwellian multimoment multispecies approaches of the terrestrial polar wind, *J. Geophys. Res.*, *105*, 2551.

Leer, E., and W. I. Axford (1972), A two-fluid solar wind model with anisotropic proton temperature, *Sol. Phys.*, *23*, 238.

Li, X. (1999), Proton temperature anisotropy in the fast solar wind: A 16 moment bi-Maxwellian model, *J. Geophys. Res.*, *104*, 19,773.

Li, X., S. R. Habbal, J. Kohl, and G. Noci (1998), The effect of temperature anisotropy on observations of Doppler Dimming and pumping in the inner corona, *Astrophys. J.*, *501*, L133.

Marsch, E., X.-Z. Ao, and C.-Y. Tu (2004), On the temperature anisotropy of the core part of the proton velocity distribution function in the solar wind, *J. Geophys. Res.*, *109*, A04102, doi:10.1029/2003JA010330.

Parker, E. N. (1963), *Interplanetary Dynamical Processes*, Wiley-Interscience, Hoboken, N. J.

Phillips, J. L., and J. T. Gosling (1990), Radial evolution of solar wind thermal electron distribution functions due to expansion and collisions, *J. Geophys. Res.*, *95*, 4217.

Pilipp, W. G., H. Miggenrieder, M. D. Montgomery, K. H. Muhlhauser, H. Rosenbauer, and R. Schwenn (1987), Characteristics of electron velocity distribution functions in the solar wind derived from the Helios plasma experiment, *J. Geophys. Res.*, *92*, 1075.

Pilipp, W. G., H. Miggenrieder, M. D. Montgomery, K. H. Muhlhauser, H. Rosenbauer, and R. Schwenn (1990), Large scale variations of thermal electron parameters in the solar wind between 0.3 and 1 AU, *J. Geophys. Res.*, *95*, 6305.

Salem, C., D. Hubert, C. Lacombe, S. D. Bale, A. Mangeney, D. E. Larson, and R. P. Lin (2003), Electron properties and Coulomb collisions in the solar wind at 1 AU: WIND observations, *Astrophys. J.*, *585*, 1147.

Schwenn, R., and E. Marsch (1990), *Physics of the Inner Heliosphere I and II*, Springer, New York.

St-Maurice, J. P., and R. W. Schunk (1976), Diffusion and heat flow equations for the mid-latitude topside ionosphere, *Planet. Space Sci.*, *25*, 907.

Velli, M. (2001), Hydrodynamics of the solar wind expansion, *Astrophys. Space Sci.*, *277*, 157.

Vocks, C., C. Salem, R. P. Lin, and G. Mann (2005), Electron halo and strahl formation in the solar wind by resonant interaction with whistler waves, *Astrophys. J.*, *627*, 540.

Withbroe, G. L. (1988), The temperature structure, mass, and energy flow in the corona and inner solar wind, *Astrophys. J.*, *325*, 442.

D. Hubert, Department of Chemistry, University of British Columbia, 2036 Main Mall, Vancouver, British Columbia, Canada V6T 1Z1. (hubert@chem.ubc.ca)

F. Leblanc, Service d'Aéronomie du CNRS/IPSL, F-91371, Verrières le Buisson, France.